Small Filters Based on Slotted Cylindrical-Ring Resonators

Reza F. Mostafavi, Dariush Mirshekar-Syahkal, *Senior Member, IEEE,* and Y. C. Mark Lim

***Abstract*—The realization of a small four-pole Chebyshev filter, using four matched slotted cylindrical-ring resonators, is explained. This filter, which does not need screws for tuning the resonators or couplings, is low-cost to manufacture and is suitable for mobile communications. The filter has a bandwidth of 75 MHz, centered at 1.73 GHz. To obtain the resonant frequency and Q-factor of the resonators as well as the coupling distances between the resonators, a new technique, the quasi-magneto-static finite-difference method, is used, which is also reported.**

***Index Terms*—Chebyshev filter, electromagnetic coupling, finite-difference technique, mobile communications, Q-factor, resonant frequency, slotted cylindrical ring resonator.**

I. Introduction

FOR ITS uniform field and high magnetic energy density within the resonator, the slotted cylindrical-ring resonator (SCR), otherwise known as the loop-gap resonator, has been used as a sample holder in nuclear magnetic resonance (NMR) measurement and electron spin resonance (ESR) spectroscopy at microwave frequencies [1], [2]. The SCR resonator has a compact structure, capable of providing medium to high Q-factors; i.e., 2000–5000. Larger Q-factors can be achieved at the expense of the size. Assuming that the SCR resonator is the wrapped-around center conductor of the combline resonator, the Q per unit volume of the former is believed to be larger than that of the latter (since for the same Q the SCR resonator should require less enclosure volume). The SCR resonator can also offer a large frequency separation between the resonant frequencies of the fundamental and the higher order modes. In view of the stated advantages, the SCR resonator seems to be a promising element for developing high-performance small filters for mobile communications.

The structure of the resonator is shown in Fig. 1(a). It is a hollow conductor cylindrical ring with a slot along its length. In practice, there is normally a cylindrical or rectangular conductor enclosure around the resonator. In the SCR resonator, the ring is equivalent to the inductor, and the slot is equivalent to the capacitor. When the length and diameter of the ring are selected appropriately and are much smaller than the wavelength at the operating frequency, the fundamental resonance and the first higher order resonance are largely separated in frequency. In a later section, this fact is shown for an SCR resonator and the result is compared with that for an equivalent combline resonator. The large frequency separation would lead to large spurious-free out-of-band response for a filter using the SCR resonator.

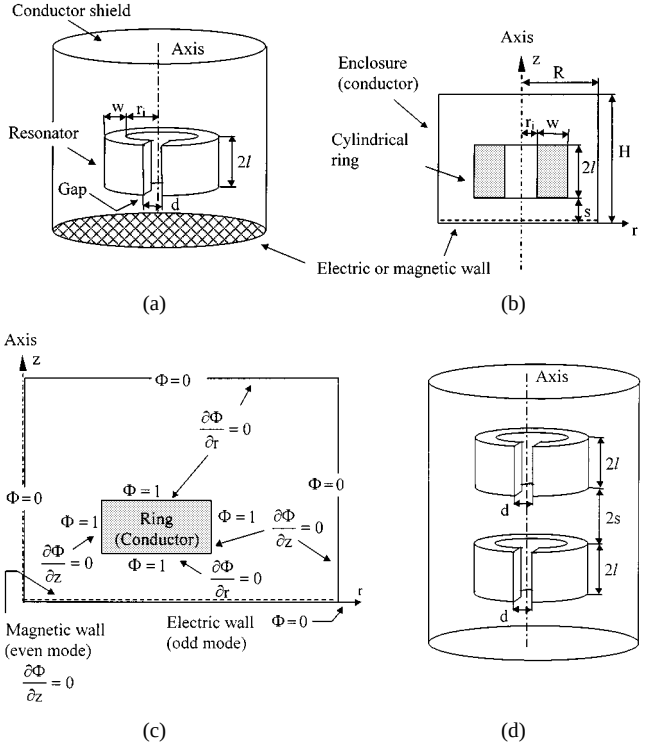

Fig. 1. (a) Slotted cylindrical ring resonator asymmetrically located within a cylindrical shield. (b) The front view of a cylindrical ring within a cylindrical shield. (c) The boundary conditions for solving (b). (d) Two coaxial (longitudinal) coupled SCR resonators within a cylindrical shield.

The design of a filter based on the SCR resonator requires a good knowledge of the resonant frequency and the Q-factor of the resonator as well as the coupling coefficients between two SCR resonators. The literature reveals that there is very limited information on the characteristics of single or coupled SCR resonators [1]–[5]. Especially for the coupled SCR resonators, there are only two sets of experimental coupling coefficients, which are for resonators with some specific dimensions [3], [5].

Very recently, based on the scalar magnetic potential and the finite-difference technique, we have developed a fast, accurate quasi-magneto-static finite-difference (QMSFD) technique for the analysis of the SCR resonator symmetrically enclosed within a cylindrical conductor shield [6]. It offers several advantages over the previous approximate closed-form

Manuscript received March 28, 2001; revised July 2, 2001. This work was supported by the Engineering and Physical Sciences Research Council (EPSRC) of the U.K. under Research Grant GR/M29801.

R. F. Mostafavi was with the Department of Electronic Systems Engineering, University of Essex, Colchester C04 3SQ, U.K. He is now with the Wireless Technologies Unit, BT, Ipswich IP5 3RE, U.K.

D. Mirshekar-Syahkal and Y. C. M. Lim are with the Department of Electronic Systems Engineering, University of Essex, Colchester C04 3SQ, U.K.

Publisher Item Identifier S 0018-9480(01)10455-2.

expressions reported in [1]–[4] for the calculation of the inductance (L), capacitance (C), resonant frequency (f), and Q-factor (Q) of the SCR resonator. By replacing the scalar magnetic potential with the stream function, we have extended the QMSFD technique for resonators, which are coaxial with the cylindrical enclosure, but asymmetrical with respect to the top and bottom wall of the shield [see Fig. 1(a)]. Also, in the modified technique, the top or bottom wall of the enclosure is allowed to be electric or magnetic, which has applications in the computation of the coupling coefficients. Details of the technique, applicable to coupled SCR resonators, are reported in [7].

This paper commences with an overview of the new QMSFD technique. Using this technique, a set of results on L, C, Q, f, and k (coupling coefficient) are presented. Then the design of a very compact four-pole Chebyshev filter with 75-MHz bandwidth and 1.73-GHz center frequency is explained. The filter has only two tuning screws for adjusting its external Q at the input and output. This supports the good accuracy of the new technique in predicting the resonant frequency and coupling coefficients as well as the low sensitivity of the filter structure to inevitable small manufacturing errors.

II. Analysis Technique

The SCR resonator is shown in Fig. 1(a). The dimensions of the resonator are normally much less than the wavelength at the fundamental resonant frequency and, since the gap of the slot is small, the resonator inductance can be computed by assuming that the slot is completely closed. Therefore, considering the inevitable shield, the structure whose inductance is to be sought is a cylindrical ring enclosed coaxially within a conductor cylinder. As shown in Fig. 1(b), the structure is rotationally symmetric, but it is not required to be axially symmetric.

As explained in our previous paper [6], when the cylindrical ring is symmetrically placed within the shield and the shield walls are all electric, the use of the scalar magnetic potential leads to an efficient computation of the magnetic field within the resonator. However, that solution becomes complex for the problem in Fig. 1(b). For the new problem, the complexity is removed by switching to the stream function, Φ, from which the field lines can be generated. Assuming the cylindrical coordinate system, Φ is related to the magnetic field components produced by current I over the ring as follows:

$$H_r = \frac{1}{r}\frac{\partial \Phi}{\partial z} \tag{1a}$$

$$H_z = -\frac{1}{r}\frac{\partial \Phi}{\partial r} \tag{1b}$$

where Φ, due to the angular symmetry of the structure, is independent of ϕ (the angle in the cylindrical coordinate system). It is not difficult to show that Φ satisfies the following differential equation:

$$\frac{\partial^2 \Phi}{\partial r^2} - \frac{1}{r}\frac{\partial \Phi}{\partial r} + \frac{\partial^2 \Phi}{\partial z^2} = 0. \tag{2}$$

Since the magnetic field is frequency-dependent, it cannot penetrate the ring and its enclosure, which are assumed to be perfect conductors. Therefore, each of these boundaries is tangent to a set of magnetic field lines. As a result, Φ in (2) has constant values at the ring and its enclosure. The boundary condition along the axis is obtained from the fact that $H_r = 0$ at $r = 0$. Using (1a), this leads to $\partial\Phi/\partial z = 0$ or $\Phi =$ constant at $r = 0$. This condition is also correct as the axis meets the top or bottom of the enclosure. Therefore, Φ on the enclosure and along the axis must have the same constant values. The boundary conditions for obtaining the even- and odd-mode inductances are shown in Fig. 1(c). Due to the angular symmetry, only half of the cross section is considered in the solution of (2).

The differential equation in (2) can be solved using the five-point finite-difference method. This technique is straightforward and can be found, for example, in [6] and [8]. However, care should be exercised when implementing the boundary conditions in the computing process [8].

The solution of (2) leads to the determination of $\mathbf{H}$ from (1). Then, the stored magnetic energy [$W = (1/2)\mu_0 \iiint_V |\mathbf{H}|^2\, dv$ where V is the volume surrounding the ring] and the dissipated power [$P = (1/2)R_s \iint_S |\mathbf{H}|^2\, ds$ where R_s is the surface resistance and S is the resonator surfaces] within the resonator, the total current flowing on the ring ($I = \oint_C \mathbf{H} \bullet d\boldsymbol{l}$ where C is the closed path tangent to the ring), and subsequently, the inductance ($L = 2W/I^2$), and the normalized Q-factor of the inductance [$Q_n = (R_s/\omega\mu_0)Q$ where $\omega = 2\pi f$], can be computed.

In conjunction with L, the slot capacitance C is required in order to compute the resonant frequency of the SCR resonator. An expression for C, based on the conformal mapping technique reported in [4], has already been modified by the authors [6], which is used in this work. The modified expression takes into account the fringing fields at the ends of the resonators. Error in the computation of C can arise if one of the resonator ends is very close to the top or bottom walls. This is not, however, of a concern, since this condition is not normally encountered in practice.

The coupling coefficient k between two coaxial identical SCR resonators (i.e., two longitudinally coupled SCR resonators) [see Fig. 1(d)] can be obtained from the expression

$$k = \frac{f_e^2 - f_m^2}{f_e^2 + f_m^2} \tag{3}$$

where f_e and f_m are the odd- and even-mode resonant frequencies [9]. Corresponding to these frequencies, capacitances and inductances are C_e and L_e, and C_m and L_m, respectively. However, as long as the two resonators are sufficiently apart, $C_e \cong C_m$. As a result, (3) reduces to

$$k = \frac{L_m - L_e}{L_m + L_e}. \tag{4}$$

The even- or odd-mode inductance of the structure in Fig. 1(d) can be evaluated by considering one of the rings while the symmetry plane between the two resonators is replaced by the magnetic or electric wall, respectively [see Fig. 1(c)]. In other words, the coupled resonator problem is reduced to a single resonator problem with appropriate boundary conditions [see Fig. 1(c)], whose solution has already been elucidated earlier in this section.

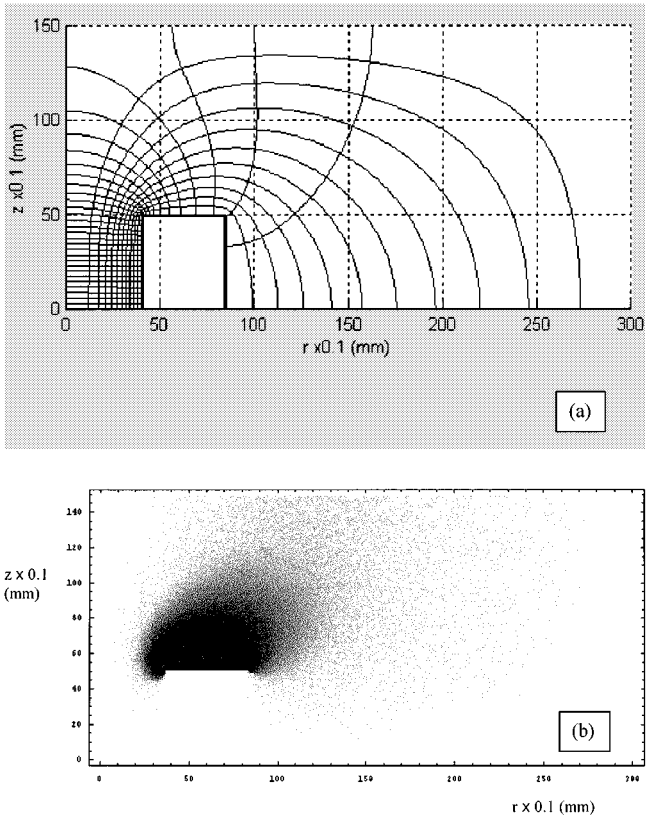

Fig. 2. (a) Lines of constant stream function and scalar magnetic potential function [6]. (b) Pictorial representation of the intensity of H_r for an SCR resonator; $w = 4$ mm, $r_i = 4.5$ mm, $l = 5$ mm, $d = 0.26$ mm, and the enclosure walls are sufficiently away from the resonators.

III. Results for Single and Coupled Resonators

Using the new QMSFD technique reported in the preceding section, various single and coupled SCR resonators were analyzed. Some results, mainly for the resonators in the filter explained in the next section, are presented in this paper.

Fig. 2(a) shows a set of lines of constant stream function and scalar magnetic potential function for an SCR resonator with $r_i = 4$ mm, $w = 4.5$ mm, $l = 5$ mm, and $d = 0.26$ mm. As expected, they are orthogonal, supporting the accuracy of the new technique based on the stream function, and our previous technique based on the scalar magnetic potential function [6]. For the same resonator, the magnetic field component H_r is presented in Fig. 2(b). From this figure and Fig. 2(a), it can be inferred that within the resonator H_z dominates and has uniform distribution, whereas near the ends of the resonator, H_r is much stronger than H_z.

In Fig. 3, C, L, and f are presented for the resonator when three out of its four dimensions are fixed at the original values and the fourth one is varied. As expected, C changes significantly with l, w, and d [see Fig. 3(a)]. The small change of C with r_i is more interesting and is merely due to the dependence of the fringing field on r_i. From Fig. 3(b), it appears that L is not very sensitive to changes in w, but it increases with r_i and decreases with l. In Fig. 3(c), the noteworthy result is the low sensitivity of f to variations in l. In this case, C and L seem to work against each other. As will be shown later, the information can be used to design resonators with the same f, but of slightly different Q.

Table I shows the theoretical and experimental resonant frequencies and Q-factors for four resonators of different materials: aluminum, brass, and silver-plated brass. One of these resonators (no. 1) is the same as the one specified earlier and, except for the gapwidth d, it shares the same dimensions with the other three. From the table (resonators nos. 3 and 4), it can be inferred that silver plating reduces the resonant frequency (due to the reduction of the gapwidth d), but increases the Q-factor. From Q and f of resonators nos. 1 and 2, it is clear that the increase of d, and hence the increase of the resonant frequency for the same resonator, leads to the enhancement of the Q-factor. This interesting effect was supported by the following approximate expression for the Q-factor of the SCR resonator:

$$Q_a = \left(\frac{\omega\mu_0\sigma}{2}\right)^{1/2} r_i \tag{5}$$

where σ is the conductivity of the resonator conductor. The derivation of (5) is based on the assumption of uniform magnetic field inside and virtually no field outside the resonator. Although it provides a good guide, (5) must be used with extreme caution and it is only valid for a limited range of resonator dimensions. Table I also reflects the results from Q_a where the measured resonant frequency has been considered in the calculation.

As seen in Table I, there are some discrepancies between the measured and theoretical values of the resonant frequencies and the Q-factors. For the resonant frequencies, the main reason is the error in the production of the slot. With normal cheap cutting techniques, at least 10% error in the size of the slot width is normal and unavoidable. As far as the Q-factors are concerned, the Q-factor of the slot (capacitor) is not considered in the theoretical evaluation of the overall Q for two reasons. It is believed that the slot Q is large and its contribution to the overall Q should not be very significant, and the expression given in [1]–[4] for the slot Q does not seem to yield correct results for all cases. Finally, some of the differences in the values of the Q-factors can be due to possible error in the value of conductivity used in the computation.

To complete the discussion on the Q-factor, the approximate expression for Q is reexamined. Q_a shows that Q can be enhanced by increasing r_i, but it does not depend on the resonator length. This is verified by the QMSFD method, using two resonators of the same frequency, but of different r_i and l. The results are shown in Table II, where the predictions are supported. As seen in Table II, Q only slightly increases with l.

To examine the occurrence of the first higher order resonance for the SCR resonator, the resonator specified earlier was isolated (i.e., no enclosure was considered in the structure) and the transmission-line matrix (TLM) technique [10], [11] was applied. As expected (since the dimensions of the resonator are much smaller than the wavelength at the fundamental resonance), the separation between the fundamental and first higher order mode is large and as shown in Fig. 4, it is about 12 GHz. The resonator is unwrapped and formed into an equivalent combline resonator with the center conductor of length $2\pi(r_i + w/2) = 39.27$ mm and with the fundamental

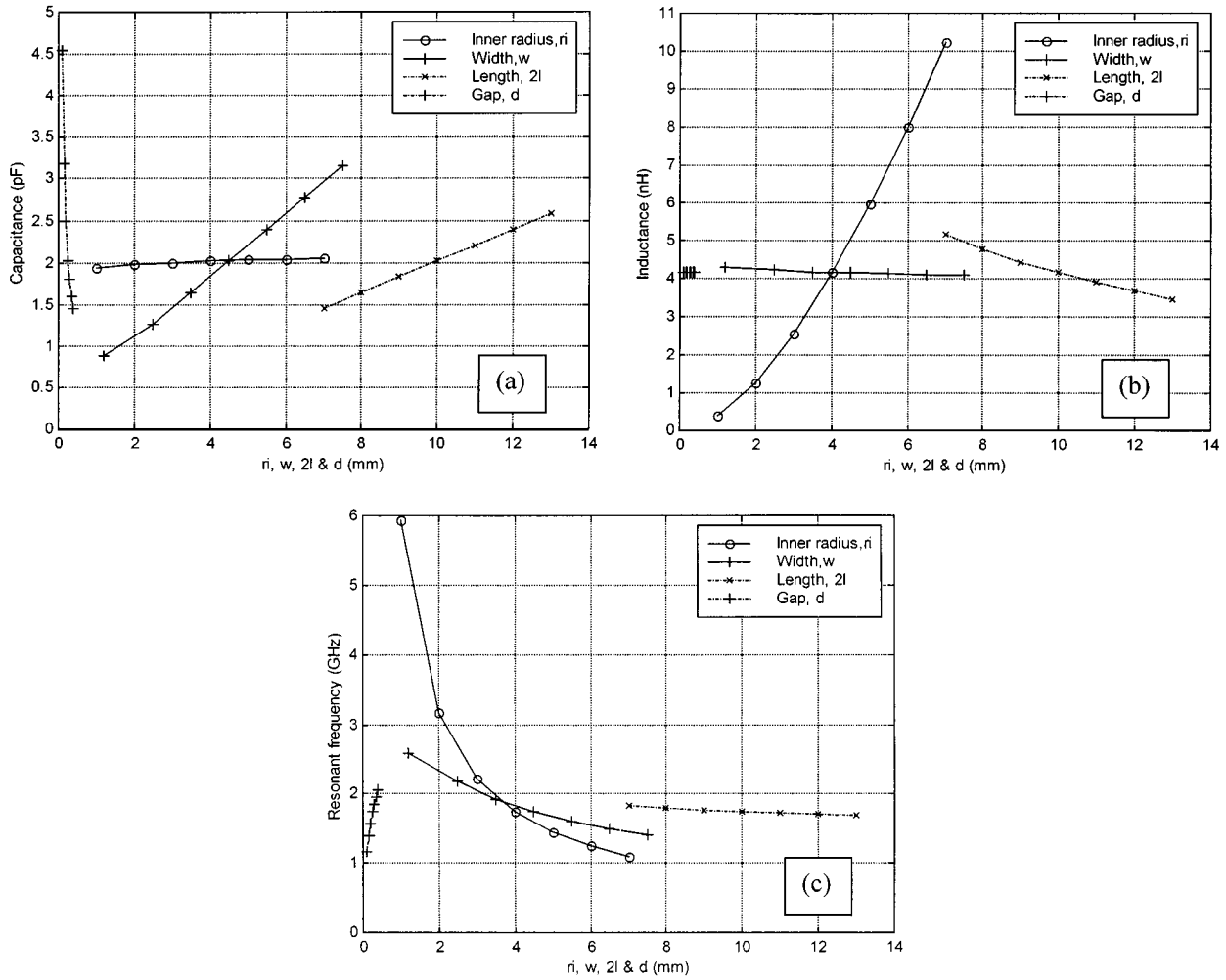

Fig. 3. Variation of: (a) the capacitance, (b) the inductance, and (c) the resonant frequency with the inner radius (r_i), width (w), length ($2l$), and gapwidth (d) of the resonator specified in Fig. 2. In these figures, three out of the four parameters are fixed at the original values and the enclosure walls are sufficiently away from the resonators.

TABLE I
THEORETICAL AND EXPERIMENTAL RESONANT FREQUENCIES AND Q-FACTORS FOR SEVERAL RESONATORS WITH DIFFERENT GAP WIDTHS AND DIFFERENT MATERIALS; $\sigma_{\text{Brass}} = 2.41 \times 10^7$ S/m, $\sigma_{\text{Silver}} = 6.12 \times 10^7$ S/m, AND $\sigma_{\text{Aluminum}} = 3.43 \times 10^7$ S/m

Res.	r_i (mm)	w (mm)	l (mm)	d (mm)	Material	f (GHz)		Q	Q_a
1	4.0	4.5	5.0	0.26	Aluminum	Theory	1.740	1761	1935
						Exp.	1.729	1319	
2	4.0	4.5	5.0	0.88	Aluminum	Theory	2.715	2167	2379
						Exp.	2.613	1604	
3	4.0	4.5	5.0	0.23	Brass	Theory	1.682	1132	1597
						Exp.	1.676	1011	
4	4.0	4.5	5.0	0.21	Silver-plated version of no. 3	Theory	1.623	2243	2509
						Exp.	1.628	2063	

resonant frequency the same as that of the SCR resonator (i.e., 1.690 GHz, see Fig. 4). The TLM simulation showed that the first higher order mode of this combline resonator is about 5.14 GHz, which is in agreement with [12]. Therefore, a filter

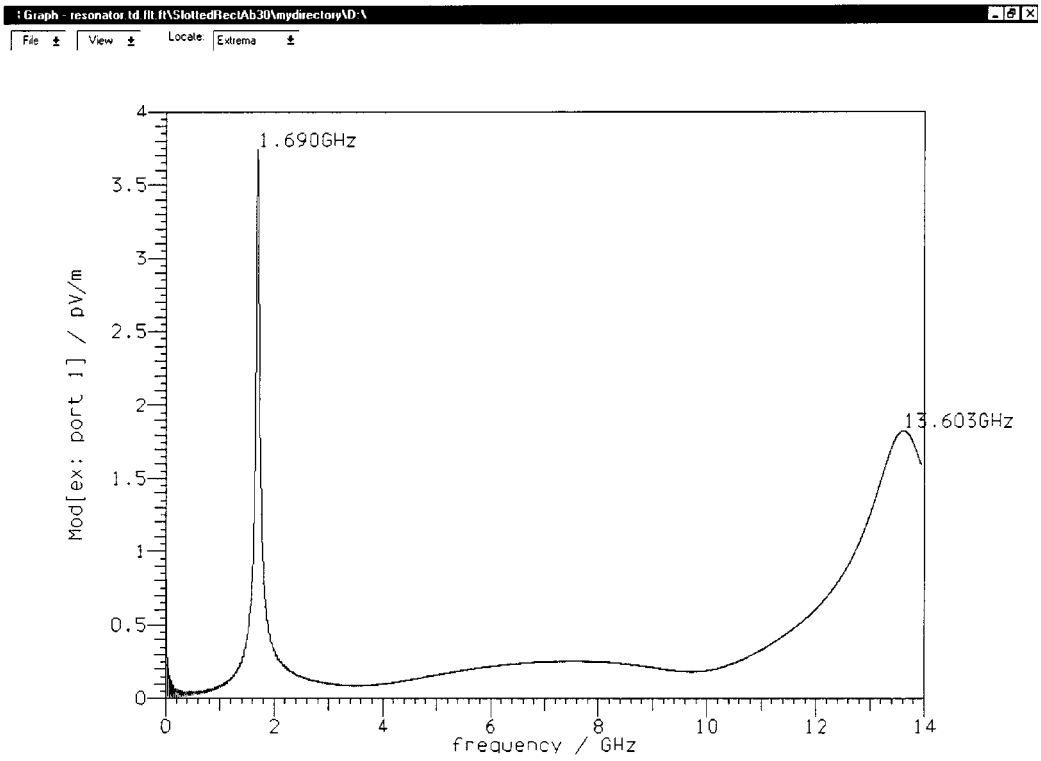

Fig. 4. The TLM computed fundamental and first higher order resonant frequencies of the SCR resonator specified in Fig. 2. In this simulation, absorbing boundary conditions are assumed at the enclosure walls.

TABLE II
EFFECTS OF THE INNER RADIUS (r_i) AND LENGTH (l) ON THE Q-FACTOR OF AN SCR RESONATOR

Res.	r_i (mm)	w (mm)	l (mm)	d (mm)	f (GHz)	Q	Q_a
1	4.0	4.5	5.0	0.26	1.740	2352	2585
2	4.0	4.5	7.5	0.29	1.741	2416	2585
3	6.0	4.5	5.0	0.23	1.741	3262	3877

using the SCR resonator is expected to exhibit a much wider band spurious-free stopband. As seen in Fig. 4, the resonant frequency of the fundamental mode (1.690 GHz) of the SCR resonator, predicted by the TLM, is about 3% lower than that (1.740 GHz) obtained by the QMSFD (see Table I). By a separate TLM simulation, it was confirmed that the difference is due to the shield in the QMSFD analysis, which reduces the stored magnetic field, thus lowering the inductance and increasing the resonant frequency. The first higher order resonant frequency can be simply estimated from the length of the resonator (longitudinal resonance). This statement is not general, since for short and wide SCR resonators the higher order resonances can be due to radial or transverse resonances. Also, as we found and it will be shown later, in filters with direct-coupled resonators, the stopband performance is dependent on the dimensions of the overall enclosure.

The results in Fig. 5 show the computed and measured coupling coefficients versus the distance, $2s$, between two coaxially (longitudinally) coupled SCR resonators [see Fig. 1(d)] with the dimensions specified earlier. The theoretical results are obtained using (4). As Fig. 5 shows, the coupling is extremely high when the distance between the two resonators is very small. The measured coupling coefficients show lower values than the predicted ones by as much as 20% for the tight spacing of $2s = 1$ mm. This can be attributed to the effect of electric coupling between the two slots and the nonuniform current distribution over the slotted cylindrical ring which have been ignored in the theoretical analysis. In fact, we have shown that, for small coupling distances, the coupling coefficient is strongly dependent on the orientation of the slots in the coupled resonators [7]. However, large couplings are not required in the design of narrow-band filters. As seen in Fig. 5, the measured coupling coefficients approach the predicted values as the spacing between the two resonators increases.

IV. FILTER

The SCR resonator specified in Section III was used to design a four-pole Chebyshev filter with 1.73-GHz center frequency, 75-MHz bandwidth, 0.1-dB ripple level, and 50-Ω impedance at terminations. In this case, from [13], the coupling coefficients were determined to be $k12 = k34 = 0.036\,025$ and $k23 = 0.028\,51$.

The resonators employed in the filter are four matched aluminum resonators with extremely small differences in their resonant frequencies. For these resonators, the theoretical and measured resonant frequencies are 1.740 GHz and 1.729 GHz, respectively. As explained before, cutting the slot close to the 0.26-mm gapwidth is difficult and hence the reason for the 0.6%

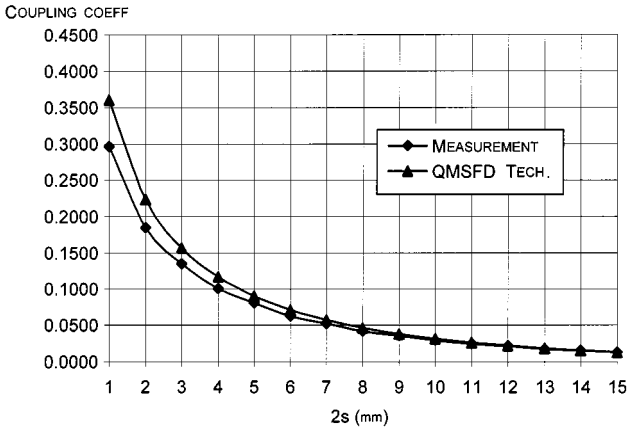

Fig. 5. Coupling coefficients versus the separation between the resonators specified in Fig. 2. The enclosure walls are sufficiently far away from the resonators.

error between theory and measurement. However, it was found that manufacturing highly matched SCR resonators is possible if correct cutting technique and tools are employed.

From Fig. 5, separation distances $2s = 8.96$ mm between the first and second resonators and between the third and the fourth resonators, and $2s = 10.12$ mm between the second and the third resonators, are required to realize the coupling coefficients. For this filter, the external Q-factor Q_e is 25.58, which has been achieved by arranging horseshoe-shaped coupling plates at the input and output of the filter.

The filter structure is shown in Fig. 6(a) and its wide- and narrow-band responses in Fig. 6(b) and (c). The interesting feature of this filter is its independence from tuning screws for the resonators and couplings between resonators, supporting the good accuracy of the theoretical technique. The only tuning screws are at the input and output for adjusting the external Q. In this case, no attempt was made to theoretically evaluate the interaction between the horseshoe coupling mechanism with the input and output resonators. The filter bandwidth and the center frequency are correctly realized and its insertion loss is about 1 dB. By silver-plating the resonators, their unloaded Q-factor increases from 1300 to about 2300 (Table I), leading to a substantially lower insertion loss. The length of this compact filter is about 100 mm.

From the responses in Fig. 6, it can be inferred that there is some fixed coupling between the input and the output probes. Also, the wide-band response indicates that the spurious-free stopband response is about 1 GHz and is not as wide as 12 GHz, which was predicted in Fig. 4 for the individual resonator. These two adverse effects are due to the enclosure and are expected to be alleviated by reducing the size or changing the shape of the enclosure. The enclosure resonances can be approximately obtained using the closed-form expressions available in electromagnetics textbooks for hollow cylindrical cavity resonators. However, for more accurate prediction of the resonances when the enclosure is loaded with the resonators, the TLM [11] or similar software packages can be used. In this case, the computation time will be very high due to the large size of the enclosure as compared to that of the SCR resonator. Research to tackle the problems is under progress.

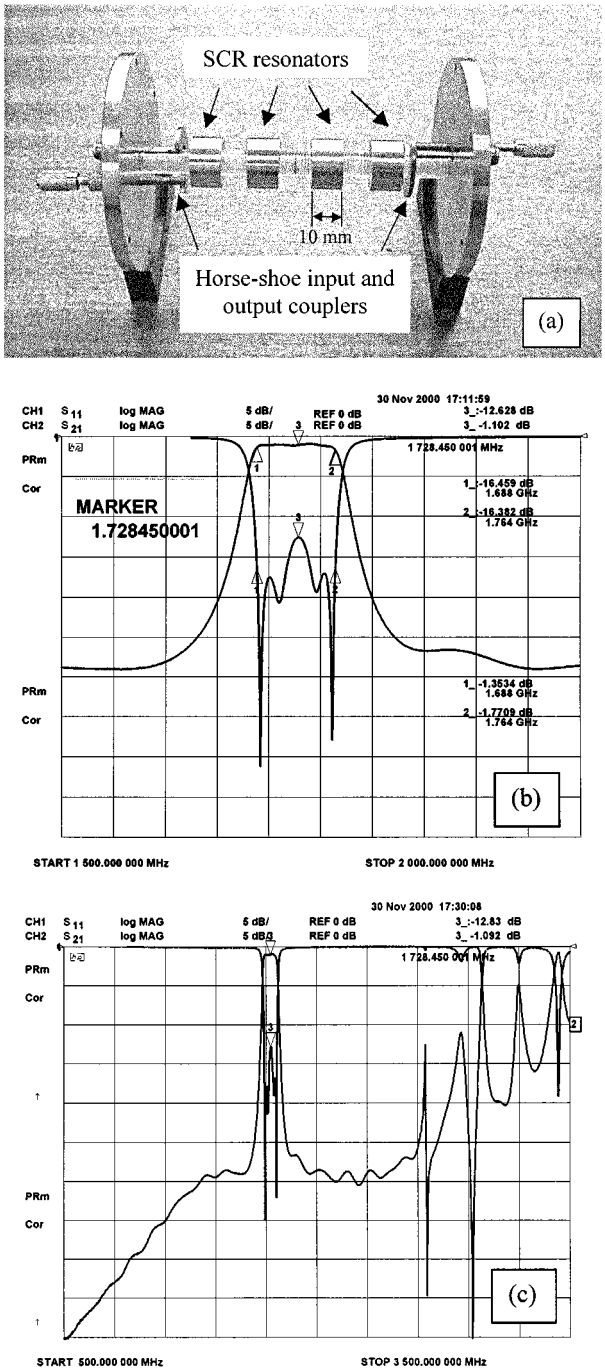

Fig. 6. (a) The structure of the filter using four matched SCR resonators specified in Fig. 2. (b) The narrow-band and (c) wide-band response of the filter.

V. CONCLUSION

For the theoretical prediction of the inductance, resonant frequency, and Q-factor of the SCR resonator, a new quasi-magneto-static technique employing the finite-difference method was reported. It was shown that this technique can be used to evaluate the coupling coefficient between two SCR resonators positioned longitudinally (coaxially). Using a set of matched aluminum resonators, a fourth-order Chebyshev filter was designed, fabricated, and tested. This compact filter, which is about 100-mm long, utilizes resonators with a maximum

dimension of 17 mm and does not require tuning. The insertion loss of the filter is about 1 dB, which is expected to improve substantially when the aluminum resonators are replaced by silver-plated resonators.

REFERENCES

[1] W. Froncisz and J. S. Hyde, "The loop-gap resonator: A new microwave lumped circuit ESR sample structure," *J. Magn. Resonance*, vol. 47, pp. 515–521, Feb. 1982.

[2] W. N. Hardy and L. A. Whitehead, "Split-ring resonator for use in magnetic resonance from 200–2000 MHz," *Rev. Sci. Instr.*, vol. 52, no. 2, pp. 213–216, Feb. 1981.

[3] M. Mehdizadeh, T. K. Ishi, J. S. Hyde, and W. Froncisz, "Loop-gap resonator: A lumped mode microwave resonant structure," *IEEE Trans. Microwave Theory Tech.*, vol. MTT- 31, pp. 1059–1063, Dec. 1983.

[4] M. Mehdizadeh and T. K. Ishi, "Electromagnetic field analysis and calculation of the resonance characteristics of the loop-gap resonator," *IEEE Trans. Microwave Theory Tech.*, vol. 37, pp. 1113–1118, July 1989.

[5] Y. Sakamoto, H. Hirata, and M. Ono, "Design of a multicoupled loop-gap resonator used for pulsed electron paramagnetic resonance measurements," *IEEE Trans. Microwave Theory Tech.*, vol. 43, pp. 1840–1847, Aug. 1995.

[6] D. Mirshekar-Syahkal, Y. C. M. Lim, and R. F. Mostafavi, "Resonant frequency of slotted ring resonator," in *Proc. 30th Eur. Microwave Conf.*, vol. 2, Paris, France, Oct. 2000, pp. 197–200.

[7] R. F. Mostafavi, D. Mirshekar-Syahkal, and Y. C. M. Lim, "Analysis of longitudinally coupled cylindrical ring resonators," *IEEE Trans. Microwave Theory Tech.*, submitted for publication.

[8] M. N. O. Sadiku, *Numerical Techniques in Electromagnetics*. Boca Raton, FL: CRC Press, 1992.

[9] K. A. Zaki and C. Chen, "Coupling of nonaxially symmetric hybrid modes in dielectric resonators," *IEEE Trans. Microwave Theory Tech.*, vol. MTT-35, pp. 1136–1142, Dec. 1987.

[10] C. Christopoulos, *The Transmission-Line Modeling Method*. Oxford, U.K.: Oxford Univ. Press, 1995.

[11] KCC Ltd, Electromagnetic Division of Flomerics, TLM House, Nottingham, NG 16 3BF, U.K, Micro-Stripes 5.5.

[12] H.-W. Wen, K. A. Zaki, A. E. Atia, and T. Dolan, "Improvement of spurious performance of combline filters," in *IEEE Microwave Theory Tech. Symp. Dig.*, 1997, pp. 1099–1102.

[13] G. Matthaei, L. Young, and E. M. T. Jones, *Microwave Filters, Impedance-Matching Networks, and Coupling Structures*. Norwell, MA: Artech House, 1980.

Reza F. Mostafavi received the B.A. degree in mathematics, the B.Eng. degree in electronics, the M.Sc. degree in telecommunications, and the Ph.D. degree from the University of Essex, Colchester, U.K, in 1981, 1990, 1991, and 1999, respectively, and the M.Sc. degree in nuclear reactor science and engineering from Queen Mary College, University of London, London, U.K., in 1982.

He joined the Department of Electronic Systems Engineering, University of Essex, in 1994, as a Senior Research Officer. From 1994 to 1999, his work concerned the research and development of a linear array system for rapid inspection of large metal surfaces, and from 1999, it concerned the study of slotted cylindrical resonators for compact microwave filters. He joined the Wireless Technologies Unit, BT Adastral Park, Ipswich, U.K., in 2001, where he is currently involved in distributed antenna systems for third-generation mobile communications.

Dariush Mirshekar-Syahkal (SM'93) received the B.Sc. degree (with distinction) in electrical engineering from Tehran University, Tehran, Iran, in 1974, and the M.Sc. degree in microwaves and modern optics and Ph.D. degree from the University College London, University of London, London, U.K., in 1975 and 1979, respectively.

From 1979 to 1984, he performed research in the characterization of millimeter-band planar transmission lines and nondestructive evaluation of metals by electromagnetic techniques at the University College London. Since 1984, he has been with the University of Essex, Colchester, U.K., where he is currently a Professor and the Head of the RF Engineering and Propagation Research Group, Department of Electronic Systems Engineering. His current research concerns problems of electromagnetic theory associated with passive microwave planar structures, including planar antennas, design of compact dielectric and conductor loaded cavity filters, and characterization of flaws in metals. He has authored numerous technical publications including *Spectral Domain Method for Microwave Integrated Circuits* (New York: Wiley, 1990).

Dr. Mirshekar is a Chartered Engineer. He is a Fellow of the Institution of Electrical Engineers (IEE), U.K.

Y. C. Mark Lim received the B.Eng. degree in electronic systems engineering (telecommunications) from the University of Essex, Colchester, U.K., in 1997, and is currently working toward the Ph.D. degree in electronic systems engineering at the University of Essex.

His principal research interests are microwave filters and electromagnetic numerical analysis.